

Kolobrodov V.G., *doc. techn. sciens, professor*
Tymchyk G.S., *doc. techn. sciences, professor*
Mykytenko V.I., *doc. techn. sciens, docent*
Kolobrodov M.S.

National Technical University of Ukraine
“Igor Sikorsky Kyiv Polytechnic Institute”
37 Peremohy Ave., Kyiv, 03056, Ukraine
e-mail: deanpb@kpi.ua

**TEST OBJECT FOR AUTOMATED
MEASUREMENT OF CHARACTERISTICS OF
POLARIZING THERMAL IMAGERS**

The growing popularity of increasing the efficiency of remote surveillance by analyzing the degree of polarization of optical radiation in the infrared spectrum requires the development of theoretical and practical methods for determining the characteristics of a new class of optoelectronic devices - polarizing thermal imagers. In contrast to the calculation methods, the issues of practical implementation of measuring benches are currently insufficiently studied. This paper proposes and analyzes options for the structure of test objects for experimental studies of polarizing thermal imagers. A metal plate is considered, which can tilt relative to the line of sight, as well as a spherical metal surface that does not require additional mechanical drives. In the former case, the degree of polarization, ellipticity, and polarization angle are varied by changing its angular orientation in the vertical and horizontal planes. The spherical surface forms a photometric body, in which the radiation of concentric zones has a certain constant degree of polarization. Such test objects provide measurements of the noise equivalent temperature difference NETD and the minimum resolvable temperature difference MRTD of polarizing thermal imagers for different polarization states of the input radiation, which is characterized by the intensity, degree of polarization, ellipticity and polarization angle. Bibl. 17, Figs. 9.

Key words: *polarizing thermal imager, test object, spatial resolution, temperature resolution, measuring bench*

Introduction

Thermal imaging surveillance systems are widely used in various fields of science and technology [1-3]. Thermal imagers can be particularly effective in the study of thermoelectric effects, which are understood as a set of physical phenomena due to the relationship between thermal and electrical processes in metals and semiconductors [4]. Thermoelectric phenomena include the Seebeck, Peltier and Thomson effects. To evaluate the efficiency of thermoelectric converters, there is a need for non-contact measurement of the static and dynamic temperature state of the converters [5].

The principle of operation of classical thermal imagers is based on the conversion of the brightness (intensity) of the radiation of the surveillance object and the background of the plane of objects into an adequate distribution of the brightness of the image of the target environment (TE) on the display screen. The limiting characteristics of such thermal imagers are determined by the radiation contrast of the TE. In recent years, developers have been actively trying to use the polarization properties of the radiation of TE

elements to significantly improve these characteristics. As a rule, radiation from the target is partially polarized, while radiation from the background is natural [3,6]. Thus, under certain conditions, polarimetric images demonstrate a significant increase in the signal from the object and suppression of background noise.

The main characteristics of polarized radiation are intensity, degree of polarization, azimuth and ellipticity of polarization [7-9]. To measure these characteristics in the infrared (IR) region of the spectrum, polarizing thermal imagers (PT) are used. At the same time, the main characteristic of any classical thermal imager is the energy resolution, which is determined by the threshold radiation contrast of the surveillance object located against the background.

To determine and measure the energy (temperature) resolution, test objects specified by the relevant standards or methods are used. There is a considerable body of monographs and papers devoted to the calculation and measurement of the energy resolution of classical thermal imagers [2, 10–12]. At the same time, there is practically no scientific and technical information on the choice of test object for modeling and measuring the main characteristics of PT. A rather important factor in the experimental determination of the characteristics of the PT at the present stage is also the possibility of automating this process, for example, in conditions of large-scale production.

Problem statement

The purpose of this paper is to substantiate the choice of a test object and develop methods for measuring the characteristics of polarizing thermal imagers. These measuring instruments must take into account the current standards for modern thermal imaging and be amenable to automation of measurement processes.

The main characteristics of thermal imagers

The generalized characteristics of thermal imagers are spatial and thermal resolution, which determine the quality of thermal imaging and temperature sensitivity. To measure the temperature sensitivity, the noise equivalent temperature difference *NETD* is used [2,10].

Polarization parameters of partially polarized radiation

Test object must assure measurement of the noise equivalent temperature difference *NETD* and minimum resolvable temperature difference *MRTD* for different polarization states of output radiation which is characterized by the intensity I_0 , polarization degree P , ellipticity χ and polarization angle θ (Fig. 1).

The process of obtaining elliptically polarized light has been considered in monographs [13–15]. The generalized equation of this type of polarization can be represented as:

$$\frac{x^2}{a^2} + \frac{y^2}{b^2} - 2\frac{x}{a}\frac{y}{b}\cos\Delta\varphi = \sin^2\Delta\varphi, \quad (1)$$

where $\Delta\varphi$ is phase difference between linearly polarized in mutually perpendicular planes components E_{0l} and E_{el} of partially polarized radiation, $x = E_0$; $a = E_{0l}$; $y = E_e$; $b = E_{el}$ are ellipse parameters.

Eq.(1) is the equation of an ellipse arbitrarily oriented relative to the optical axis 00 of the crystal (phase plate) (Fig.1). The orientation of the ellipse is determined by the polarization angle θ , and the shape of the ellipse is determined by the angle of ellipticity χ . Depending on these angles, elliptically polarized light is converted into linearly polarized light, as well as circularly polarized light with rotation of the resulting vector $\vec{E}_r = \vec{E}_o + \vec{E}_e = \vec{x} + \vec{y}$ to the right or left.

In the general case, the ellipse (1) is located inside a rectangle of size $2E_{0l} \times 2E_{e1}$ and touches its contour at four points (Fig. 1). If the third term in Eq.(1) is zero, then the axes of the ellipse are parallel to the χ and y axes.

The polarization angle θ is the angle between the main axis of the ellipse and the horizontal axis x , which is determined by the components of the electric field of light:

$$\operatorname{tg} 2\theta = \frac{2E_{0x}E_{0y} \cos \Delta\varphi}{E_{0x}^2 + E_{0y}^2}, \text{ де } 0 < \theta < \pi. \quad (2)$$

The angle of ellipticity χ is given by the ratio of the lengths of the minor and major axes of the ellipse:

$$\operatorname{tg} \chi = \frac{\pm b}{a}, \text{ де } -\pi/2 < \chi < \pi/2 \quad (3)$$

The angle of ellipticity χ is also determined by the components of the electric field of light:

$$\operatorname{tg} 2\chi = \frac{2E_{0x}E_{0y} \cos \Delta\varphi}{E_{0x}^2 + E_{0y}^2}, \text{ де } 0 < \theta < \pi. \quad (4)$$

Polarization of thermal radiation

Studies of the laws of thermal radiation of heated objects indicate that metal surfaces have a higher degree of radiation polarization compared to dielectric and transparent surfaces. The greatest degree of polarization is observed in the radiation of polished surfaces when observed at a large angle relative to the normal to the surface. This is due to the laws of refraction of radiation at the "metal - air" boundary.

According to Kirchhoff's law, the spectral emissivity $\varepsilon(\lambda)$ of the surface of the observed object, which is in a state of temperature equilibrium, is equal to the absorption coefficient $\alpha(\lambda)$ and is related to the reflection coefficient $R(\lambda)$ by the relation:

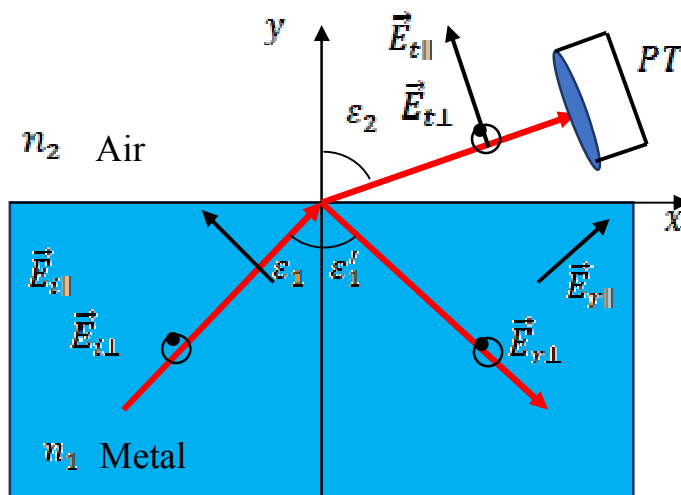


Fig. 2. Radiation and reflection of light incident at an inclined angle ε_1 from metal to the "metal - air" boundary

$$\varepsilon(\lambda) = \alpha(\lambda) = 1 - R(\lambda). \quad (7)$$

The amplitude of thermal radiation E_t at the “metal-air” boundary is partially polarized, where the parallel component $E_{\varepsilon_{\parallel}}$ is greater than the perpendicular component $E_{\varepsilon_{\perp}}$ (Fig. 2). The axis of sight (observation) of PT is located in the xy plane of observation.

Using Kirchhoff’s law (7) and Fresnel’s formulae for partial energy reflection coefficients R_{\parallel} and R_{\perp} [15, 16], we obtain formulae for calculating the parallel and perpendicular components of (partial) radiation coefficients

$$\varepsilon_{\parallel} = \left| \frac{E_{t_{\parallel}}}{E_{i_{\parallel}}} \right|^2 = \frac{4n_1 \cos \varepsilon_2}{\cos \varepsilon_2 + 2n_1 \cos \varepsilon_2 + n_1^2 + \kappa_1^2}, \quad (8)$$

$$\varepsilon_{\perp} = \left| \frac{E_{t_{\perp}}}{E_{i_{\perp}}} \right|^2 = \frac{4n_1 \cos \varepsilon_2}{(n_1^2 + \kappa_1^2) \cos \varepsilon_2 + 2n_1 \cos \varepsilon_2 + 1}, \quad (9)$$

where $n_c = n_1 - j\kappa_1$ is a complex refractive index of metal; ε_2 is refracting (viewing) angle. The resulting emissivity is the average of the parallel and perpendicular components

$$\varepsilon = \frac{1}{2}(\varepsilon_{\parallel} + \varepsilon_{\perp}). \quad (10)$$

The degree of polarization of radiation is defined as

$$DOP(\varepsilon_v) = \frac{\varepsilon_{\perp}(\varepsilon_v) - \varepsilon_{\parallel}(\varepsilon_v)}{\varepsilon_{\perp}(\varepsilon_v) + \varepsilon_{\parallel}(\varepsilon_v)}, \quad (11)$$

where $\varepsilon_v = \varepsilon_2$ is viewing angle.

The dependences of partial emissivity factors $\varepsilon_{\parallel}(\varepsilon_v)$ and $\varepsilon_{\perp}(\varepsilon_v)$ and the degree of polarization $DOP(\varepsilon_v)$ at the “aluminum-air” boundary on the viewing angle ε_v are shown in Figs. 3 and 4. For the radiation of the aluminum surface, the perpendicular component is larger than the parallel component. The perpendicular component increases with increase in viewing angle to a maximum value of about 0.92, and then decreases at large angles. The perpendicular component decreases monotonically with increase in angle ε_v . The overall emissivity factor ε increases slightly with increase in angle ε_v . The degree of polarization with increase in viewing angle increases to a maximum value of 92% at $\varepsilon_v \approx 90^\circ$. When constructing plots to take into account the roughness and oxidation of the surface of the aluminum plate, the complex refractive index $n_c = 4.45 - j3.3$ was used.

On the contrary, for the “dielectric-air” boundary, the partial components of the emissivity factor decrease with increase in viewing angle. The overall emissivity factor decreases with increase in viewing angle in proportion to $\cos \varepsilon_v$. The degree of polarization of the surface radiation also increases with increase in the angle ε_v , but has a smaller value compared to the radiation of the surface of metals.

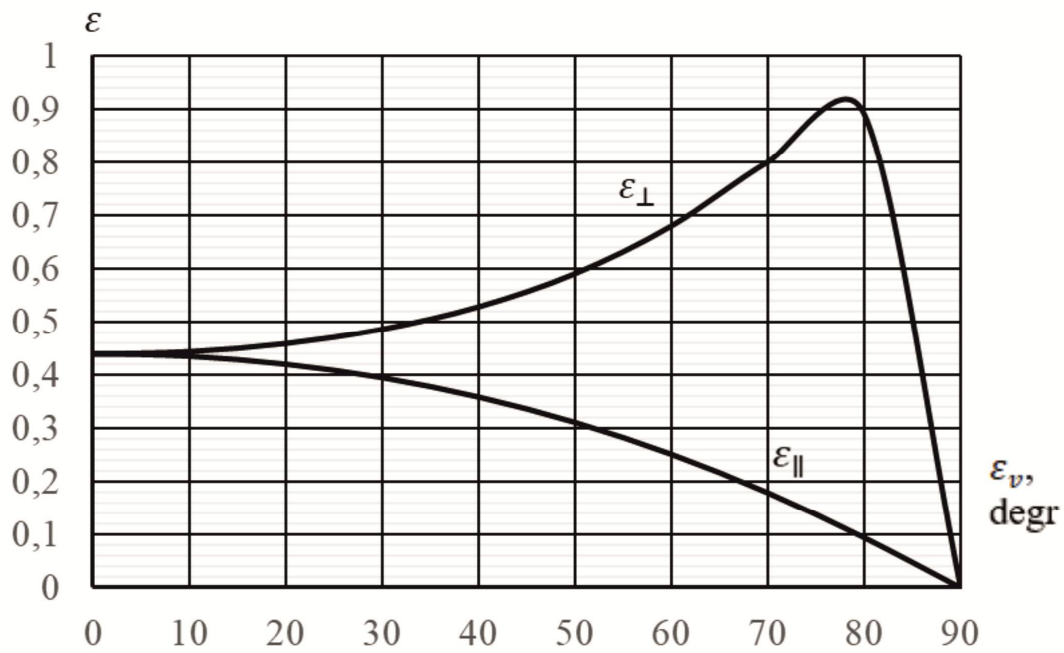


Fig. 3. Dependences of partial emissivity factors of the aluminum surface on the angle ϵ_v at $n_c = 4,45 - j3,3$

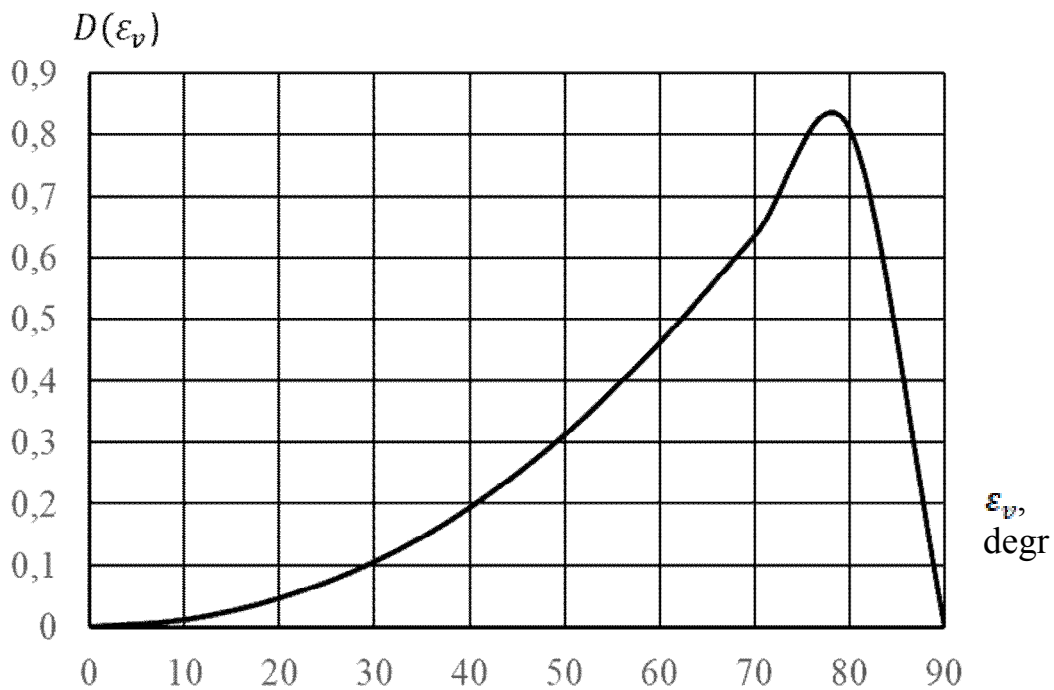


Fig. 4. The dependence of the degree of polarization of the radiation of the aluminum surface on the viewing angle ϵ at $n_c = 4,45 - j3,3$

Thus, the analysis of the laws of thermal radiation of the metal surface shows the following:

1. The radiation is partially polarized, which is due to the difference in emissivity factors for linearly polarized light in surveillance plane ϵ_{\parallel} and the plane ϵ_{\perp} perpendicular to it,
2. The parallel component of linearly polarized radiation $E_{\parallel}(\epsilon_v)$ in surveillance plane with increase in viewing angle monotonically decreases from 0.44 at $\epsilon_v = 0^\circ$ to zero at $\epsilon_v = 90^\circ$.
3. The perpendicular component of linearly polarized radiation $E_{\perp}(\epsilon_v)$ in surveillance plane with increase in viewing angle ϵ_v increases from 0.44 to maximum value 0.92 at $\epsilon_v \approx 80^\circ$, and then decreases to zero at at $\epsilon_v = 90^\circ$.
4. The degree of polarization $DOP(\epsilon_v)$ of radiation of aluminum surface with increase in viewing angle ϵ_v increases from zero to maximum value 0.83 at $\epsilon_v \approx 80^\circ$ and decreases to zero at $\epsilon_v = 90^\circ$.
5. For small viewing angles $\epsilon_v < 30^\circ$, which is characteristic of typical surveillance cases, the degree of polarization does not exceed 10%, and the resulting emissivity factor is $\approx \epsilon_{\parallel} \approx \epsilon_{\perp} = 0,438$

Selection of test object

For experimental studies of classical thermal imagers and measurement of their characteristics, test objects are used, which are located on a uniform background [9,10]. The schematic of a setup for measuring the characteristics of PT is shown in Fig.5. The schematic of a setup for measuring the characteristics of the PT is shown in Fig. 5. The background emitter 1, the test object 2, and the studied polarizing thermal imager 3 are successively located on the optical bench [17].

As a background, it is proposed to use a metal (aluminum) plate covered with black lacquer, which has an emissivity factor close to one. Therefore, such a plate will be considered as a completely black body, the surface of which radiates according to Lambert's law. The rear surface of the background plate is covered with thermoplastic. There is a heater between the thermoplastic and the aluminum plate, and thermocouples for temperature measurement in the four corners of the plate. This ensures a uniform temperature background.

The heater allows changing the surface temperature of the plate in a given range. The plate is located perpendicular to the optical axis of the PT. In this case, the radiation entering the PT from the background, will be unpolarized, i.e. $P_b \approx 0$ (Fig. 4). This is characteristic of most natural background sources of IR radiation.

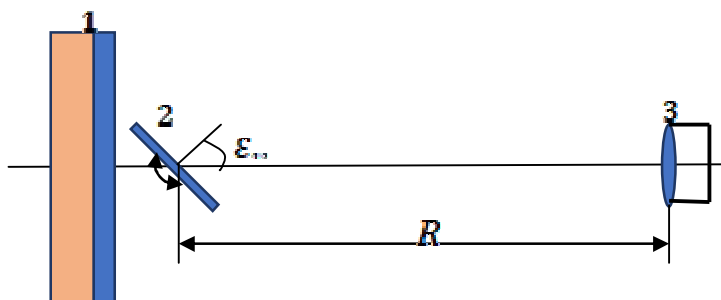


Fig. 5. Schematic of the method for measuring the NETD of a polarizing thermal imager (in the horizontal plane): 1 - background emitter; 2 – test object; 3 - polarizing thermal imager

As test object 2, it is proposed to use a rectangular plate, the Foucault gauge or a spherical surface made of aluminum with a complex refractive index $n_c = n - j\kappa$, which are located perpendicular to the optical axis of the PT.

To measure the *NETD*, we will use a rectangular plate that can rotate about the vertical axis by the viewing angle ε_v relative to the optical axis of the PT in the horizontal plane. By changing the angle ε_v , a change in the degree of polarization $P(\varepsilon_v)$ of the radiation entering the PT is achieved (Fig. 4). The test object rotates about the vertical axis in the range from 0° to 80° . The temperature of the plate is equal to the ambient temperature and is measured by temperature sensors.

The change of the polarization angle θ is achieved by tilting (reversing) the plate relative to the vertical plane of the optical system (Fig. 6).

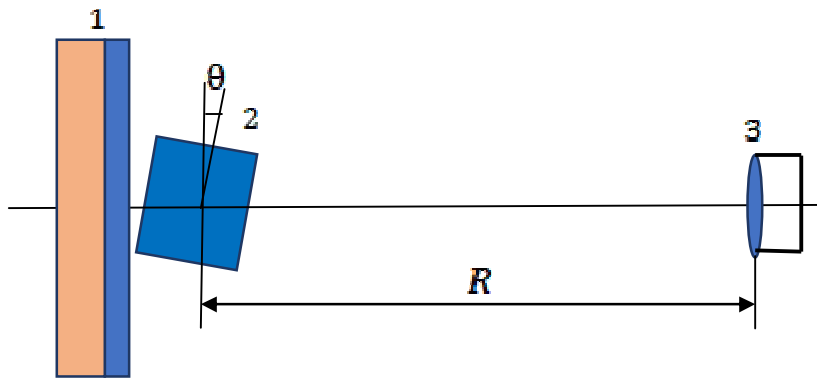


Fig. 6. Schematic of the method for measuring the *NETD* of a polarizing thermal imager at different polarization angles θ (in the vertical plane): 1 – background emitter; 2 – test object; 3 – polarizing thermal imager

The technical implementation of the test object turns can be quite simple and allows automating the measurement process.

To study the dependence of the *NETD* on the degree of polarization, it is proposed to use a hemisphere made of aluminum. A certain point on the hemisphere surface will correspond to a variable angle ε_v between the beam entering the PT and the normal to the surface, i.e. each point of the hemispheric image has its own degree of polarization (Fig. 7).

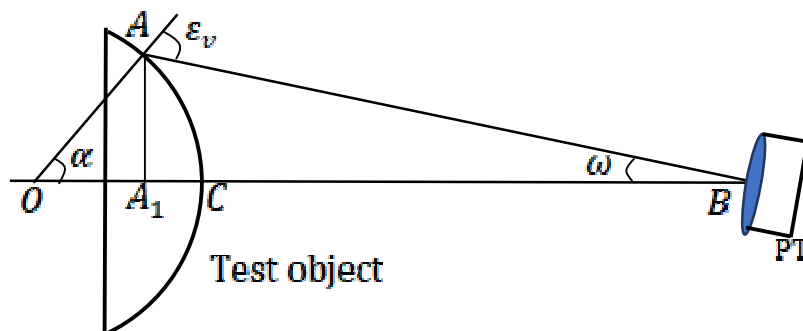


Fig. 7. Schematic for measuring PT characteristics using a test object with a spherical surface.

Let us determine the dependence of the viewing angle ε_v of the surface of test object on the deviation angle ω of the PT optical axis from the horizontal plane using Fig. 7. From the triangle ABO we have $\varepsilon_v = \alpha + \omega \rightarrow \alpha = \varepsilon_v - \omega$. From the triangles AA_1O and AA_1B we get

$$AA_1 = AO \sin \alpha = A_1B \operatorname{tg} \omega, \quad (12)$$

where $AO = r_{th}$ is radius of the spherical surface of test object; $A_1B = BC + CA_1 = R + CA_1$, where $BC = R$ is the distance from PT to test object.

From the triangle AA_1O we have $OA_1 = r_{th} \cos \alpha$. Then $CA_1 = OC - OA_1 = r_{th}(1 - \cos \alpha)$. Let us substitute the obtained relations to Eq.(12)

$$r_{th} \sin \alpha = (R + CA_1) \operatorname{tg} \omega = [R + r_{th}(1 - \cos \alpha)] \operatorname{tg} \omega$$

We write the obtained transcendental equation in the form

$$\sin \alpha = [R_n + (1 - \cos \alpha)] \operatorname{tg} \omega, \quad (13)$$

where $R_n = R/r_{th}$ is the normalized distance from the PT to the test object.

The solution of Eq. (13) are the dependences of the viewing angle $\varepsilon_v = \alpha + \omega$ on the change in the direction ω of the optical axis of thermal imager for different values of the normalized distance from the PT to the test object R_n , which are shown in Fig.8.

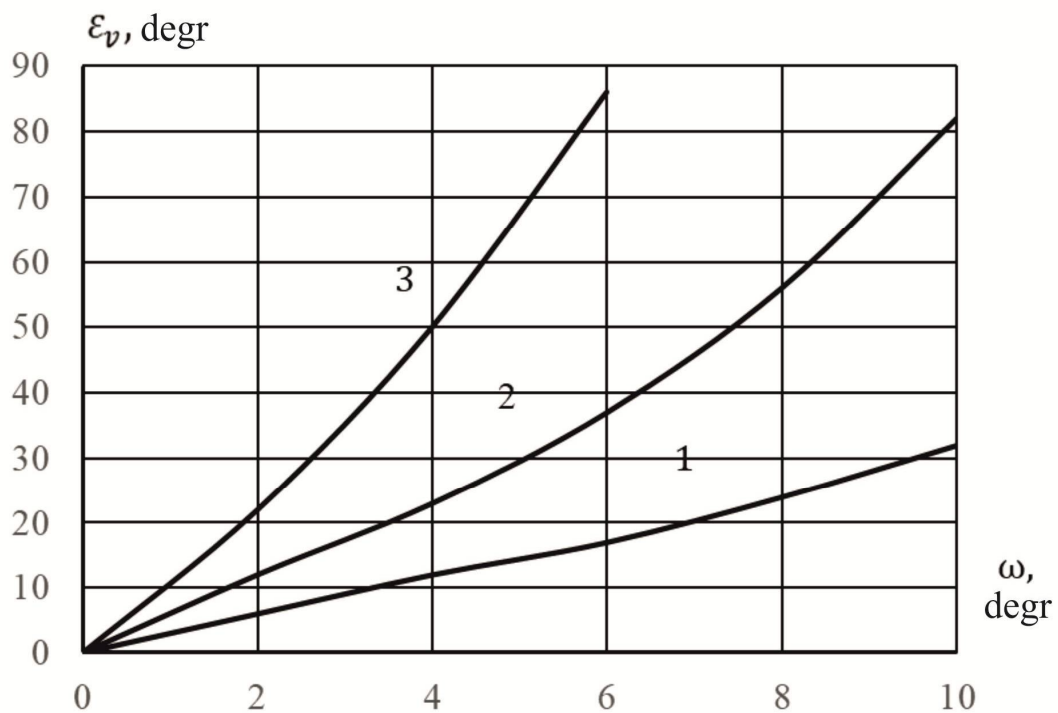


Fig. 8. Dependence of the thermal imager viewing angle ε_v of the test object spherical surface on the deviation angle ω of the PT optical axis from the horizontal plane for different values of the normalized distance from the PT to the test object R/r_{th} : 1–2; 2–5; 3–10

The emitter in the form of a spherical surface can be used to form particles of polarized radiation with different degrees of polarization. The degree of polarization will be determined by formula (11), the plot of which is shown in Fig. 4. The angular position ω of a point on the surface of a sphere, which corresponds to a certain degree of polarization, is found from the relation $DOP(\omega) = DOP(\varepsilon_v - \alpha)$.

The dependence of the deviation angle ω of the PT optical axis on the angle ε_v is determined from Eq. (13), or the plots shown in Fig. 8. In turn, the degree of polarization $DOP(\omega)$ is found from the plot shown in Fig. 4. The calculated dependence $DOP(\omega)$ is given in Fig. 9.

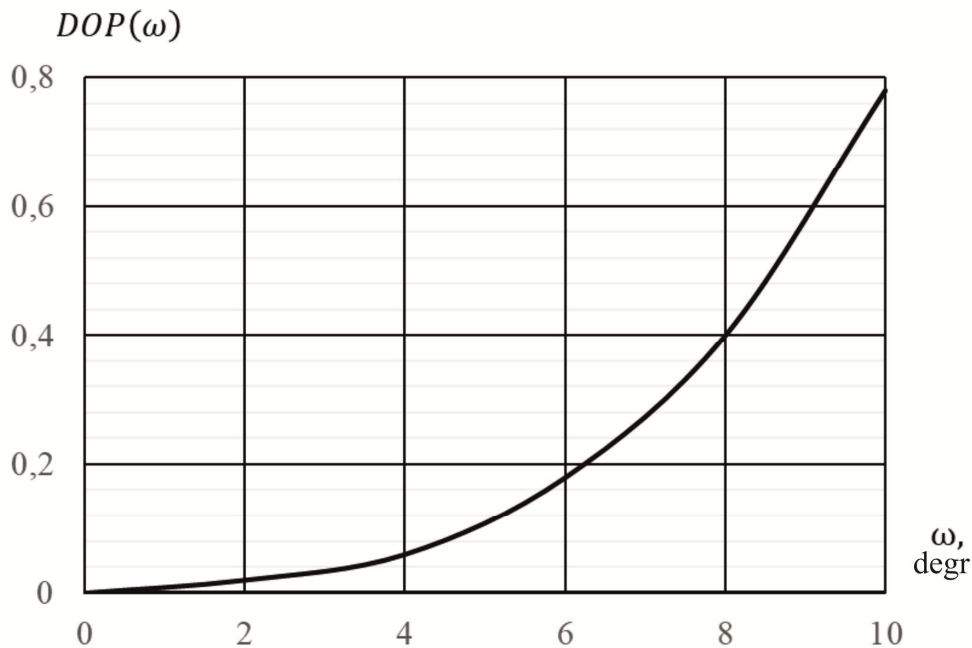


Fig. 9. Dependence of the degree of polarization $DOP(\omega)$ of the spherical surface radiation on the angle of deviation ω of the PT optical axis for the normalized distance from the PT to the test object $R/r_{th} = 5$

The analysis of the obtained dependence indicates the following:

1. If the optical axis of the PT coincides with the optical axis of the experimental setup, i.e. when $\omega = 0$, the degree of radiation polarization in the centre of the image of the test object is zero.
2. With a deviation of the optical axis of PT from the optical axis of the setup by the angle ω , the degree of polarization increases from zero to the maximum value 0.83 for the normalized distance from the test object $R/r_{th} = 5$.

To measure the minimum resolving temperature difference of PT, it is reasonable to use in the schematic shown in Fig.5 the test object in the form of a four-mark Foucault gauge [6,7].

Conclusions

1. A feature of the test object for measuring polarization characteristics is the ability to generate partially polarized IR radiation with the given intensity, temperature contrast, polarization degree, ellipticity and polarization angle.
2. Physical models of the test object are proposed in the form of a rectangular metal plate for measuring *NETD*, a metal plate in the form of the Foucault gauge for measuring *MRTD* and a metal spherical surface.

3. The plates allow one to change the degree of polarization, ellipticity and polarization angle by changing their angular orientation in the vertical and horizontal planes.
4. A spherical surface makes it possible to obtain an image of such a surface, the concentric zones of which are formed by radiation having a certain constant degree of polarization.

References

1. Peri'c Dragana, Livada Branko, Peri'c Miroslav and Vuji' Saša (2019). Thermal imager range: predictions, expectations, and reality. *Sensors*, 19, 3313.
2. Schuster Norbert, Kolobrodov Valentin G. (2004). *Infrarotthermographie*. Zweite, überarbeitete und erweiterte Ausgabe. Berlin: WILEY-VCH.
3. Vollmer Michael and Mollman Klaus-Peter (2018). *Infrared thermal imaging. Fundamentals, research and applications*. 2nd ed. Weinheim: Wiley – VCH.
4. Anatychuk L.I. (2020). Efficiency criterion of thermoelectric energy converters using waste heat. *J. Thermoelectricity*, 4, 59-63.
5. Anatychuk L.I., Vikhor L.M., Kotsur M.P., Kobylanskyi R.R., Kadenyuk T.Ya. (2016). Optimal control of time dependence of cooling temperature in thermoelectric devices. *J. Thermoelectricity*, 5, 5-11.
6. Vollmer M., Karstadt S., Mollmann K.-P., Pinno F. (2001). *Identification and suppression of thermal imaging. InfraMation Proceedings*. Brandenburg: University of Applied Sciences. Brandenburg. – ITC 104 A.
7. Goldstein D.H. (2011). *Polarized light*. Third edition. London New York: CRC Press is an imprint of Taylor & Francis Group.
8. Gurton K.P., Yuffa A.J., Videen G.W. (2014). Enhanced facial recognition for thermal imagery using polarimetric imaging. *Optical Society of America*, 39(13), 3857–3859.
9. Zhang Y., Shi Z.G., Qiu T.W. (2017). Infrared small target detection method based on decomposition of polarization information. *Journal of Electronic Imaging*, 33004, № 1.
10. Chrzanowski K. (2010). *Testing thermal imagers. Practical guidebook*. Military University of Technology, 00-908 Warsaw, Poland.
11. Kaplan Herbert. (2007). *Practical applications of infrared thermal sensing and imaging equipment*. 3d ed. Washington: SPIE Press.
12. Chyzh I., Kolobrodov V., Molodyk A., Mykytenko V., Tymchyk G., Romaniuk R., Kisała P., Kalizhanova A., Yeraliyeva B. (2020). Energy resolution of dual-channel opto-electronic surveillance system. *SPIE Proceedings*, 11581, Photonics Applications in Astronomy, Communications, Industry, and High Energy Physics Experiments 2020; 115810K.
13. Chipman Russell A., Tiffany Lam Wai-Sze, Young Garam (2019). *Polarized light and optical systems*. Taylor & Francis, CRC Press.
14. Collett Edward (2005). *Field guide to polarized light*. Washington: SPIE Press.
15. Born M., Wolf E. (2002). *Principles of optics*. 7th ed. Cambridge: Cambridge University.
16. Kolobrodov, V.G. Polarization model of thermal contrast observation objects / Kolobrodov, V.G., Mykytenko, V.I., Tymchyk, G.S. // *Journal of thermoelectricity*. - 2020, 2020(1). – P. 36–49.
17. Short N. J., Yuffa A.J., Videen G. and Hu S. (2016). Effects of surface materials on polarimetric thermal measurements: applications to face recognition. *Applied Optic*, 55 (19), 5226–5233.

Submitted 29.04.2021

Колобродов В.Г., докт. техн. наук, професор
Тимчик Г.С., докт. техн. наук, професор
Микитенко В.І., докт. техн. наук, доцент
Колобродов М.С.

Національний технічний університет України
«Київський політехнічний інститут імені Ігоря Сікорського»
проспект Перемоги, 37, Київ, 03056, Україна
e-mail: deanpb@kpi.ua

ТЕСТ-ОБ'ЄКТ ДЛЯ АВТОМАТИЗОВАНОГО ВИМІРЮВАННЯ ХАРАКТЕРИСТИК ПОЛЯРИЗАЦІЙНИХ ТЕПЛОВІЗОРІВ

Зростаюча популярність підвищення ефективності дистанційних спостережень за рахунок аналізу ступеню поляризації оптичного випромінювання в інфрачервоному діапазоні спектру вимагає розроблення теоретичних і практичних методів визначення характеристик нового класу оптико-електронних приладів – поляризаційних тепловізорів. На відміну від розрахункових методів питання практичної реалізації вимірювальних стендів наразі опрацьовані недостатньо. В даній статті запропоновано і проаналізовано варіанти структури тест-об'єктів для експериментальних досліджень поляризаційних тепловізорів. Розглянуто металеву пластину, що може нахилитись відносно лінії візування, а також сферичну металеву поверхню, яка не потребує додаткових механічних приводів. В першому випадку ступінь поляризації, еліптичність і поляризаційний кут варіюються шляхом зміни її кутової орієнтації у вертикальній і горизонтальній площині. Сферична поверхня формує фотометричне тіло, в якому випромінювання концентричних зон має певну постійну ступінь поляризації. Такі тест-об'єкти забезпечують вимірювання еквівалентної шуму різниці температур і мінімальної роздільної різниці температур поляризаційних тепловізорів для різних станів поляризації вхідного випромінювання, яке характеризується інтенсивністю, ступенем поляризації, еліптичністю і поляризаційним кутом. Бібл. 17, рис. 9.

Ключові слова: поляризаційний тепловізор, тест-об'єкт, просторове розділення, температурне розділення, вимірювальний стенд

Колобродов В.Г., докт. техн. наук, професор
Тимчик Г.С., докт. техн. наук, професор
Микитенко В.І., докт. техн. наук, доцент
Колобродов М.С.

Национальный технический университет Украины
"Киевский политехнический институт имени Игоря Сикорского»,
проспект Победы, 37, Киев, 03056, Украина, *e-mail: deanpb@kpi.ua*

ТЕСТ-ОБЪЕКТ ДЛЯ АВТОМАТИЗИРОВАННОГО ИЗМЕРЕНИЯ ХАРАКТЕРИСТИК ПОЛЯРИЗАЦИОННЫХ ТЕПЛОВИЗОРОВ

Возрастающая популярность повышения эффективности дистанционных наблюдений за счет анализа степени поляризации оптического излучения в инфракрасном диапазоне спектра требует разработки теоретических и практических методов определения характеристик нового класса оптико-электронных приборов – поляризационных тепловизоров. В отличие от расчетных методов вопросы практической реализации измерительных стендов в настоящее время проработаны недостаточно. В данной статье предложены и проанализированы варианты структуры тест-объектов для экспериментальных исследований поляризационных тепловизоров. Рассмотрена металлическая пластина, которая может наклоняться относительно линии визирования, а также сферическую металлическую поверхность, не требующая дополнительных механических приводов. В первом случае степень поляризации, эллиптичность и поляризационный угол варьируются путём изменения ее угловой ориентации в вертикальной и горизонтальной плоскости. Сферическая поверхность формирует фотометрическое тело, в котором излучение концентрических зон имеет определенную постоянную степень поляризации. Такие тест-объекты обеспечивают измерение эквивалентного шума разности температур и минимального раздельного различия температур поляризационных тепловизоров для разных состояний поляризации входного излучения, характеризующееся интенсивностью, степенью поляризации, эллиптичностью и поляризационным углом. Библ. 17, рис. 9.

Ключевые слова: поляризационный тепловизор, тест-объект, пространственное разделение, температурное разделение, измерительный стенд

References

1. Perić Dragana, Livada Branko, Perić Miroslav and Vujić Saša (2019). Thermal imager range: predictions, expectations, and reality. *Sensors*, 19, 3313.
2. Schuster Norbert, Kolobrodov Valentin G. (2004). *Infrarotthermographie*. Zweite, überarbeitete und erweiterte Ausgabe. Berlin: WILEY-VCH.
3. Vollmer Michael and Mollman Klaus-Peter (2018). *Infrared thermal imaging. Fundamentals, research and applications*. 2nd ed. Weinheim: Wiley – VCH.
4. Anatyshuk L.I. (2020). Efficiency criterion of thermoelectric energy converters using waste heat. *J. Thermoelectricity*, 4, 59-63.
5. Anatyshuk L.I., Vikhor L.M., Kotsur M.P., Kobylanskyi R.R., Kadenyuk T.Ya. (2016). Optimal control of time dependence of cooling temperature in thermoelectric devices. *J. Thermoelectricity*, 5, 5-11.
6. Vollmer M., Karstadt S., Mollmann K.-P., Pinno F. (2001). *Identification and suppression of thermal imaging*. *InfraMation Proceedings*. Brandenburg: University of Applied Sciences. Brandenburg. – ITC 104 A.
7. Goldstein D.H. (2011). *Polarized light*. Third edition. London New York: CRC Press is an imprint of Taylor & Francis Group.
8. Gurton K.P., Yuffa A.J., Videen G.W. (2014). Enhanced facial recognition for thermal imagery using polarimetric imaging. *Optical Society of America*, 39(13), 3857–3859.

9. Zhang Y., Shi Z.G., Qiu T.W. (2017). Infrared small target detection method based on decomposition of polarization information. *Journal of Electronic Imaging*, 33004, № 1.
10. Chrzanowski K. (2010). *Testing thermal imagers. Practical guidebook*. Military University of Technology, 00-908 Warsaw, Poland.
11. Kaplan Herbert. (2007). *Practical applications of infrared thermal sensing and imaging equipment*. 3d ed. Washington: SPIE Press.
12. Chyzh I., Kolobrodov V., Molodyk A., Mykytenko V., Tymchyk G., Romaniuk R., Kisała P., Kalizhanova A., Yeraliyeva B. (2020). Energy resolution of dual-channel opto-electronic surveillance system. *SPIE Proceedings*, 11581, Photonics Applications in Astronomy, Communications, Industry, and High Energy Physics Experiments 2020; 115810K.
13. Chipman Russell A., Tiffany Lam Wai-Sze, Young Garam (2019). *Polarized light and optical systems*. Taylor & Francis, CRC Press.
14. Collett Edward (2005). *Field guide to polarized light*. Washington: SPIE Press.
15. Born M., Wolf E. (2002). *Principles of optics*. 7th ed. Cambridge: Cambridge University.
16. Kolobrodov, V.G. Polarization model of thermal contrast observation objects / Kolobrodov, V.G., Mykytenko, V.I., Tymchyk, G.S. // *Journal of thermoelectricity*. - 2020, 2020(1). – P. 36–49.
17. Short N. J., Yuffa A.J., Videen G. and Hu S. (2016). Effects of surface materials on polarimetric thermal measurements: applications to face recognition. *Applied Optic*, 55 (19), 5226–5233.

Submitted 29.04.2021